

Coronagraph Technology Assessment

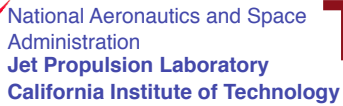
Domenick Tenerelli
Lockheed Martin Space Systems Company

Rémi Soummer
AMNH

May 28, 2008

Coronagraph Technology

- Internal Coronagraph Requirements
- Coronagraph Masks
- Mirror Technology
- Deformable Mirrors
 - John Trauger's Team Developments
 - Material Science Considerations
 - Cost
- Thermal
- Isolation Systems
- Coatings, Dichroics and Beam Splitters
- Detectors



Technology Criticality & Milestones

[illegible]

ASMSC Exoplanet Infrastructure Support



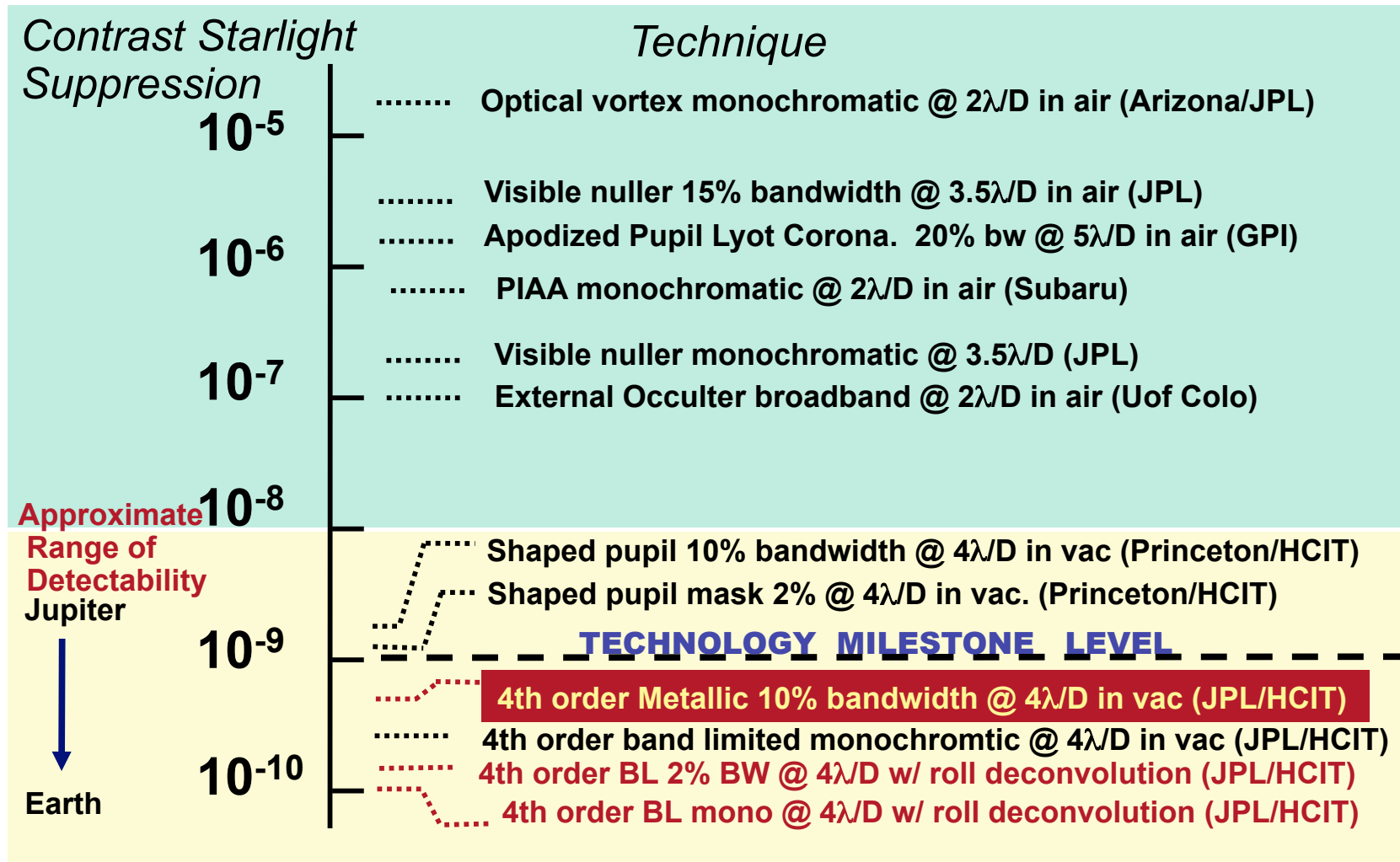
ExoPlanet Exploration Program

Astrophysics Strategic Mission Concept Studies - Exoplanet Science					
6 Coronagraphs out of 19 Selected Concepts = 32%					
Name	Instrument	Size	PI Affiliation	Category	Infrastructure Support Requested
PECO Pupil-mapping Exoplanet Coronagraph Observer	PIAA	1.4m Telescope Medium Class	Olivier Guyon Univ of Arizona	Internal Coronagraph	<ul style="list-style-type: none"> • HCIT Demo • Detector Expertise • WFSC infrastructure (nulling algorithm, DMs) • Modeling infrastructure (testbed verification, spectral characterization, orbit determination, integrated modeling) • Fabrication of PIAA occulting masks
ACCESS	Band-Limited Dielectric, PIAA, Shaped-Pupil, Vortex, 4QPM	1.5m Telescope Medium Class	John Trauger JPL		<ul style="list-style-type: none"> • HCIT Demo for each coronagraph technology: Band-limited, Shaped-Pupil, PIAA, Vector Vortex • WFSC infrastructure (2-DM nulling algorithm, additional DMs) • Fabrication of metallic & dielectric masks
XPC eXosolar Planet Characterization	Hybrid: Internal / External	4m Flagship w/ 30m Shade	David Spergel Princeton		<ul style="list-style-type: none"> • Fabrication of External Occulting masks • Modeling infrastructure (integrated modeling, diffraction modeling for occulter tolerancing, GNC, navigation & completeness optimization)
NWO New Worlds Observer	External Occulter	4m Flagship w/ 25m/50m Shade	Webster Cash - Univ of Colorado	External Coronagraph	No support requested
DAVINCI	Dilute Aperture Visible Nuller	4x1.2m Flagship	Mike Shao JPL	Internal Coronagraph / Interferometer	<ul style="list-style-type: none"> • Vacuum testing of components • DM calibration • PSF calib w/ 4 beam nuller • Modeling Infrastructure Support
EPIC	Visible Nuller	Medium Class	Mark Clampin - GSFC		
Planet Hunter	Astrometric Interferometer	Medium Class	Geoff Marcy UC Berkeley	Interferometer	None required

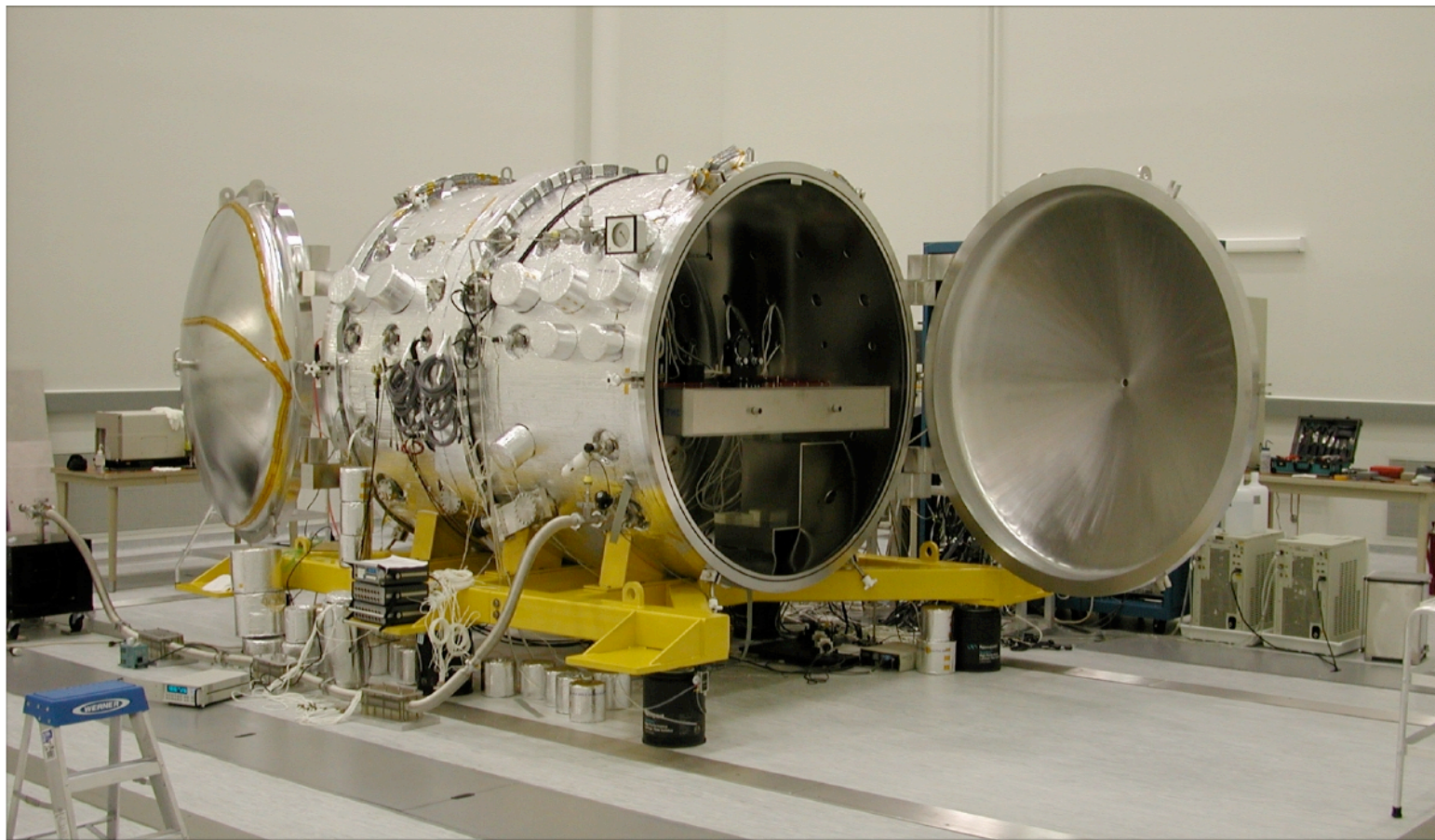
Coronagraph Technology Status April 2008 Starlight Suppression Laboratory Results



ExoPlanet Exploration Program

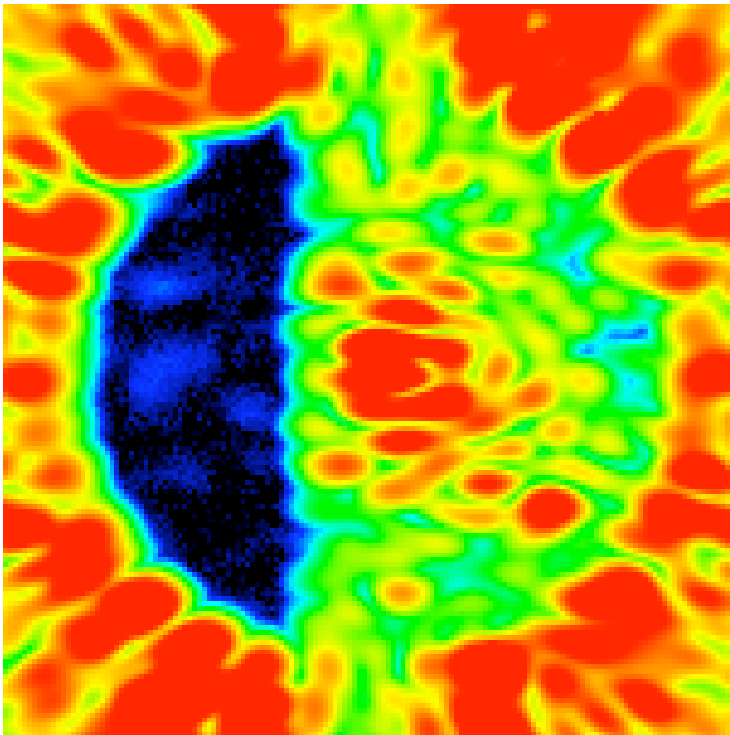


High Contrast Imaging Testbed at JPL



HCIT JPL testbed results

Contrast in 760-840 nm (10%) bandwidth

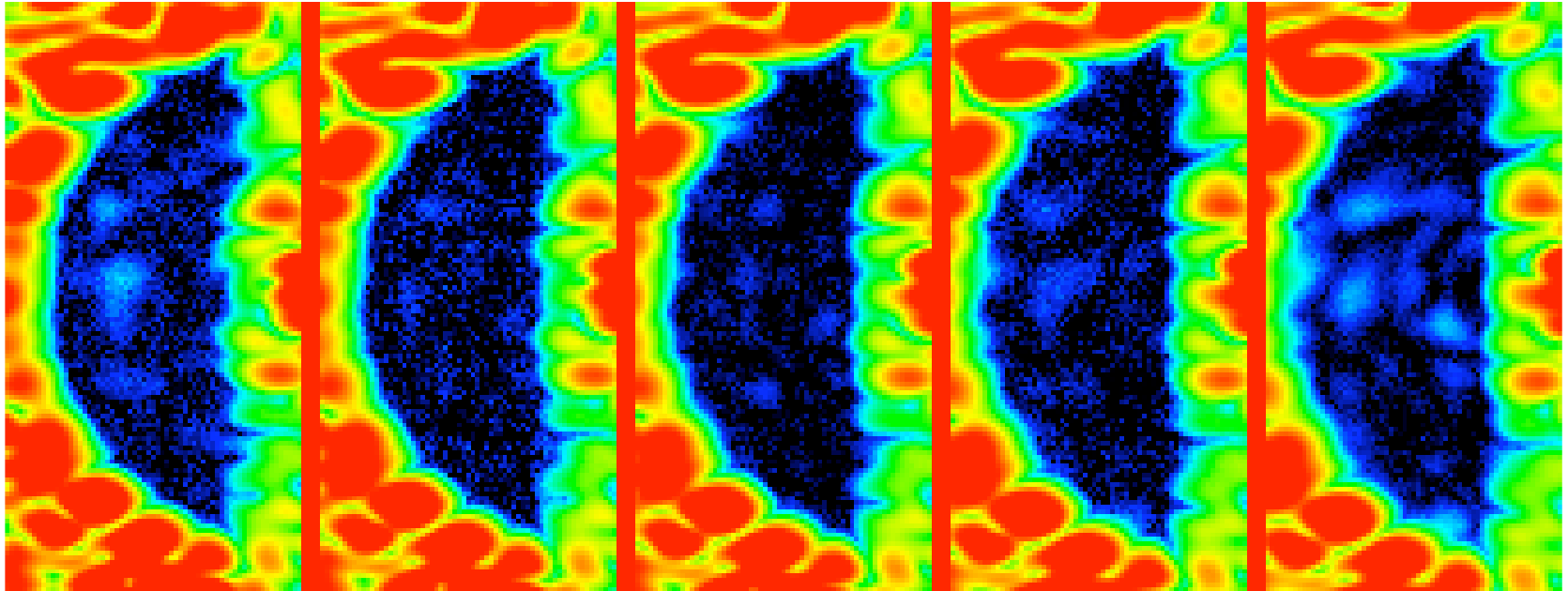


Contrast averaged across five multi-wavelength EFC iterations over a 5 hour period:

Inner 4-5 λ/D box:
 $C = 5.2 \text{ e-}10$

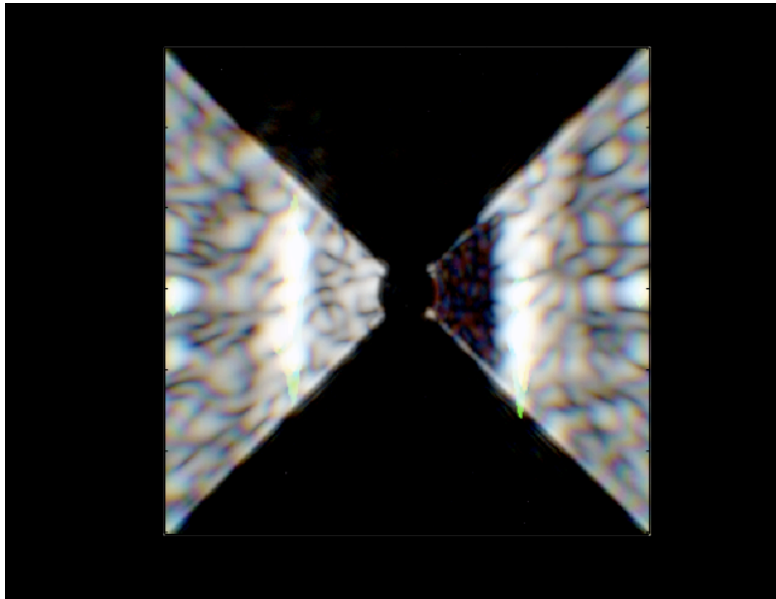
Outer 4-10 λ/D box:
 $C = 7.5\text{e-}10$

Contrast across five contiguous 2% passbands

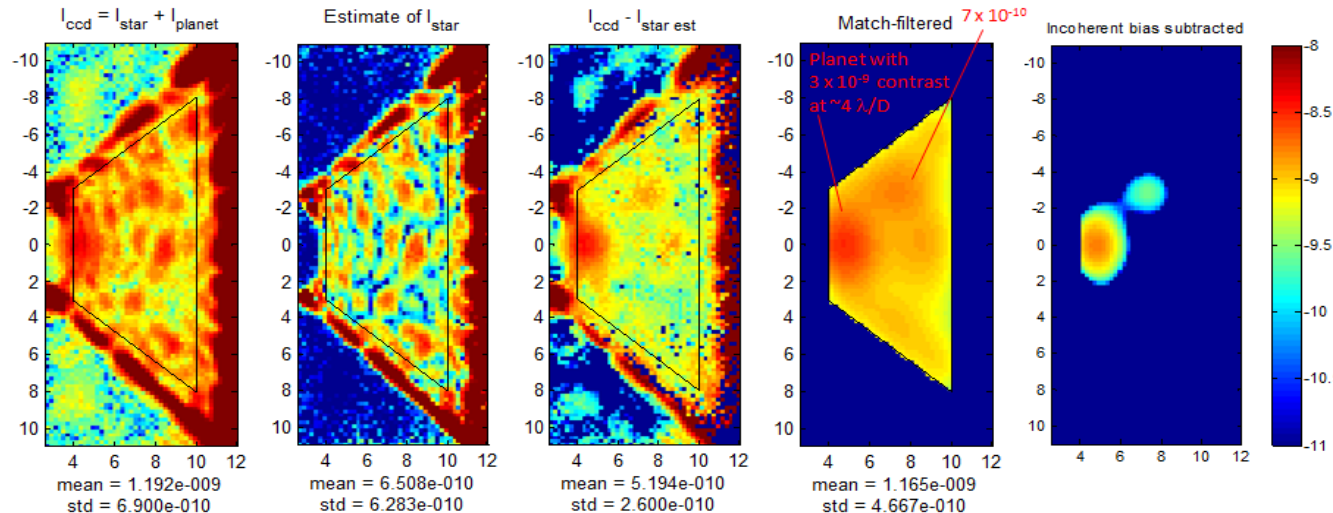


	768 nm	784 nm	800 nm	816 nm	832 nm
C(4-5)	9.8e-10	6.7e-10	6.5e-10	3.9e-10	3.2e-10
C(4-10)	11.5e-10	6.3e-10	5.2e-10	6.2e-10	11.4e-10

Shaped Pupils



Best suppression achieved with Shaped Pupils:
 2.4×10^{-9} contrast at $4 \lambda/D$
from 760-840nm.



Mask Fabrication technologies

- Amplitude masks (continuous, half tone techniques)
 - *phase & chromaticity of the phase*
- Phase masks
 - *Focal plane (4QC, OVC)*
- Etching (DRIE)
 - *Shaped pupils, Lyot Stops*
- Aspheric polishing / etching
 - *PIAA, Phase plate coronagraph*

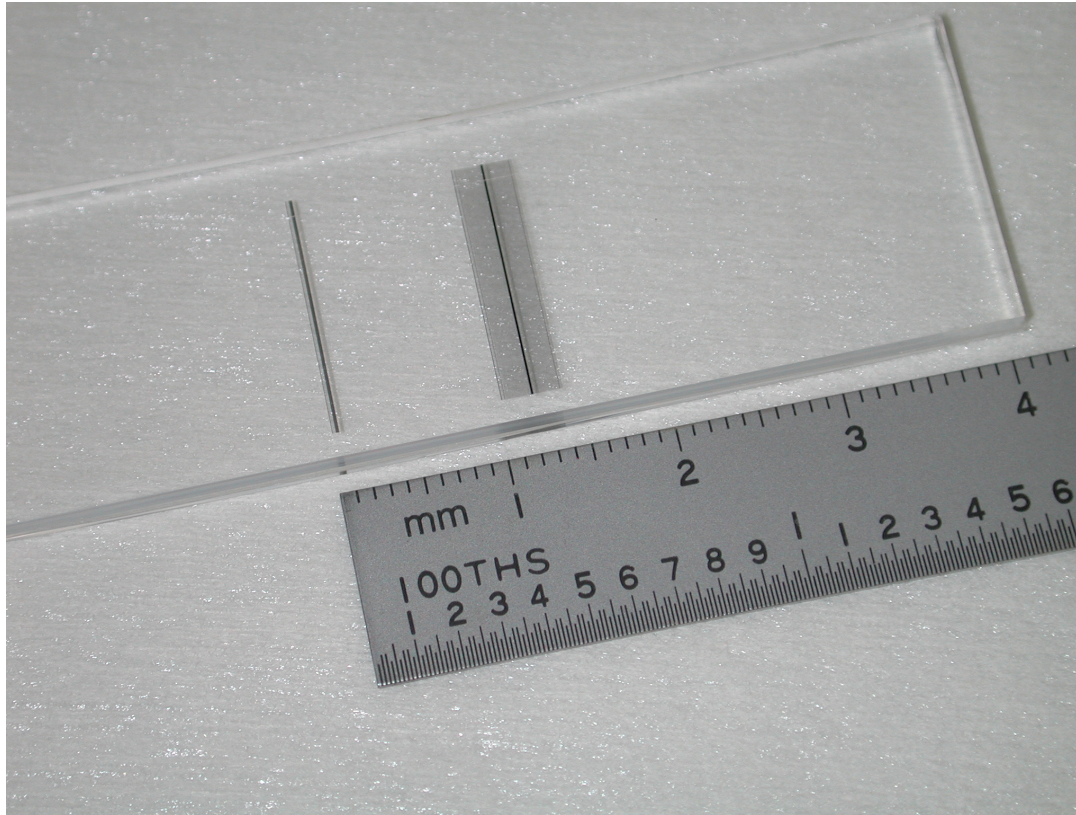
Mask Fabrication technologies

Predicted coronagraph contrast with metal and metal-dielectric masks

Example	Configuration	Bandwidth ($\delta\lambda / \lambda$)	C (4-5 λ/D) $\times 10^{-10}$	C (4-10 λ/D) $\times 10^{-10}$	ϵ	Lyot throughput
1	HEBS IK89	10%	4.1	1.5	0.47	42.4%
2	Nickel	10%	3.7	1.4	0.36	55.1%
3	Ni + MgF ₂	10%	0.38	0.76	0.26	67.2%
4	Ni + MgF ₂	20%	3.7	3.8	0.26	67.2%
5	Ni + MgF ₂	30%	5.1	6.0	0.27	66.0%

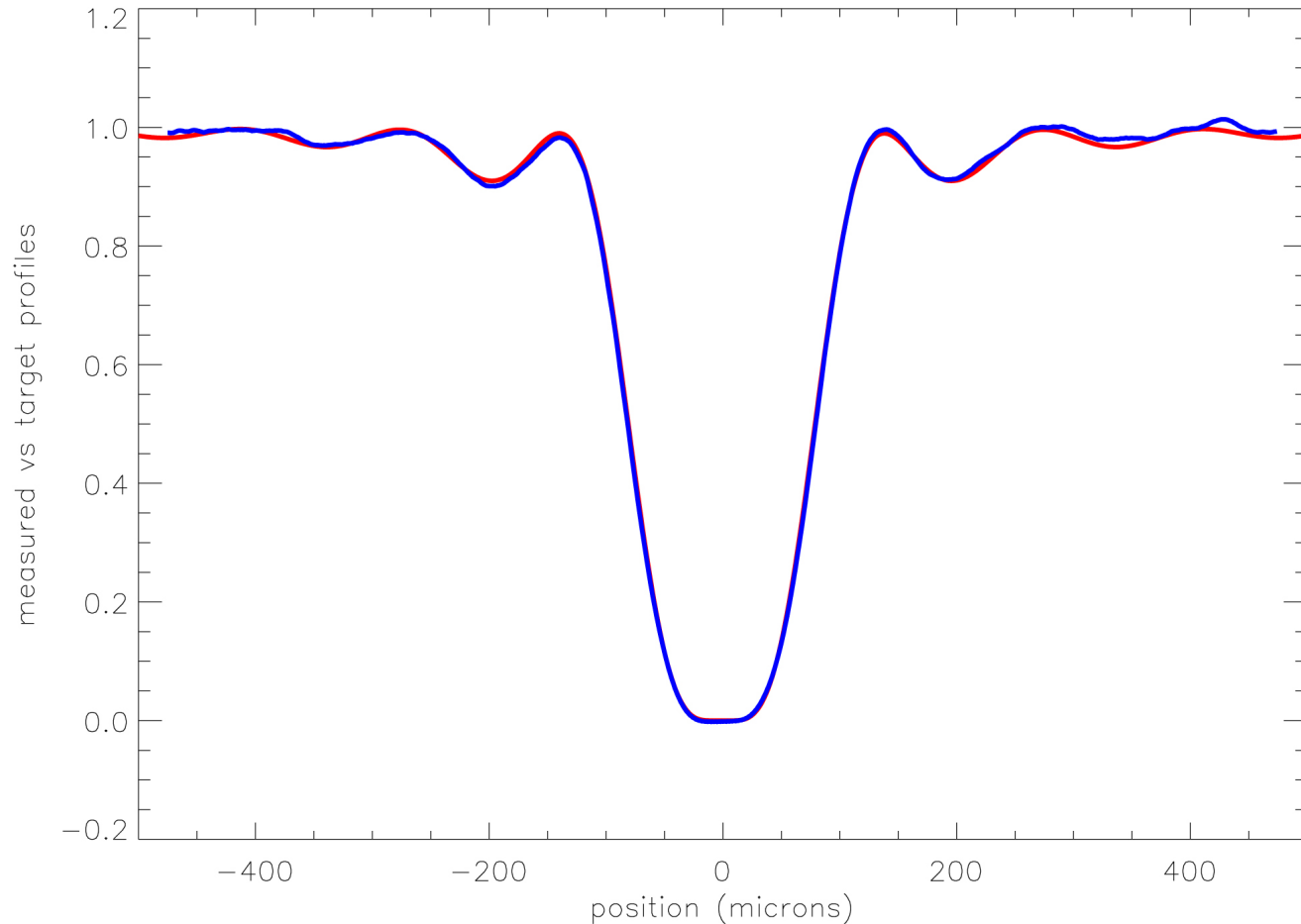
Predicted contrast, bandwidth, and throughput for the nickel occulter, with comparisons to metal/dielectric and HEBS, from Moody & Trauger (2007).

Metallic mask for April 2008 experiments



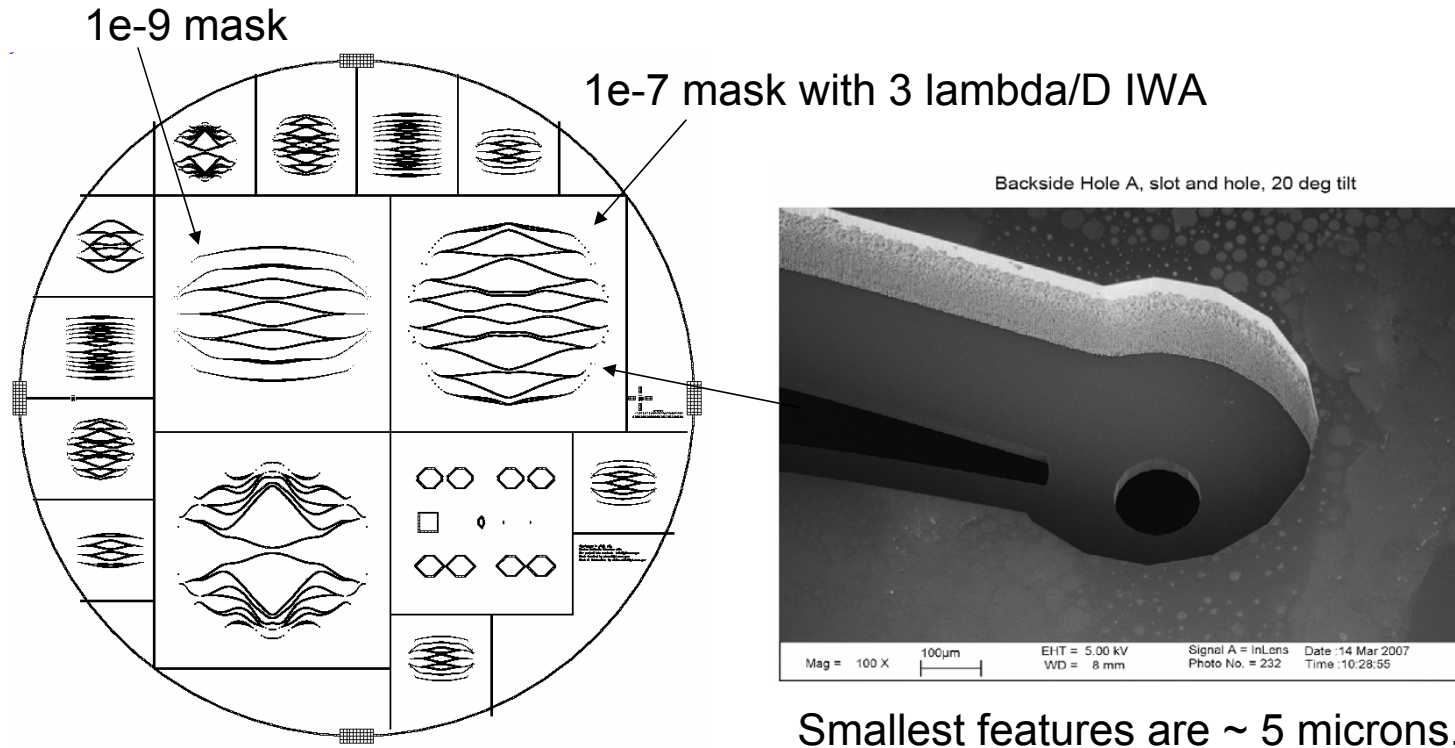
Nickel occulter (fabricated 1/15/08) vacuum-deposited on a fused silica substrate. Occulter is the linear pattern at right, at left is a calibration pattern.

Metallic mask for April 2008 experiments



Comparison of the intensity transmittance profiles as **specified** (red) and as **measured** (blue) in the 080115 deposition run.

Etching



Silicon-on-Insulator wafers.
DRIE process. 2-sided etching.
Manufactured at JPL Microdevices Laboratory

A process is designed for making a $1e-10$ free-standing mask, but not demonstrated yet.

Mission size	Small	Large
Lyot Coronographs	Models generated using conventional Fourier calculations have been validated versus HCIT for bandlimited occulters to contrasts of $\sim 5\text{e-}10$ in broadband light.	Models expected to work accurately down to $1\text{e-}10$ contrast and better, but have not been fully validated. Polarization is a concern. Simulations for a TPF-like system with wavefront control have been run.
Shaped Pupils	Models validated versus HCIT. Conventional Fourier methods can be used with some additional input from analytical calculations to accurately handle the narrow parts of the masks.	Vector propagation analysis comes into play at $<1\text{e-}10$ contrasts. Ability to work with wavefront control in broadband light at these levels has not yet been shown. Tiny mask defects are important at these contrasts.
Phase Masks	Models have not been validated below $1\text{e-}6$ - $1\text{e-}7$ contrast. Most techniques cannot be accurately implemented with conventional Fourier techniques with some additional analytical input due to sharp phase discontinuities. Scattering effects from sharp edges are not easy to model.	Little work has been done to verify models to $1\text{e-}10$ contrast level, and no work with integrating the models with wavefront control to investigate broadband performance with aberrations present.

Mission Size	Small	Large
PIAA	Cannot accurately model using straightforward techniques, especially with wavefront errors present. Need to integrate ray tracing and propagation. Models have not been validated to anywhere near 1e-9 contrast.	Accurate modeling at 1e-10 levels with aberrations and wavefront control appears daunting, and no complete and efficient method of propagation has been proposed (approximations have been suggested, but they require additional apodization of the system to avoid calculating some diffraction effects, and thus are incomplete models).
Occultor		Models have not been validated to anywhere close to 1e-10 contrasts. Modeling small errors on the occultor requires non-Fourier methods that compute piecemeal propagation. Hybrid concepts have not modeled systems with occulter+wavefront errors with control.
Visible Nuller	Models have not been verified below ~1e-6 contrast. Effects of fibers, if used, cannot be accurately modeled with conventional Fourier techniques.	No model validation, integration of wavefront control at these levels has not been demonstrated.

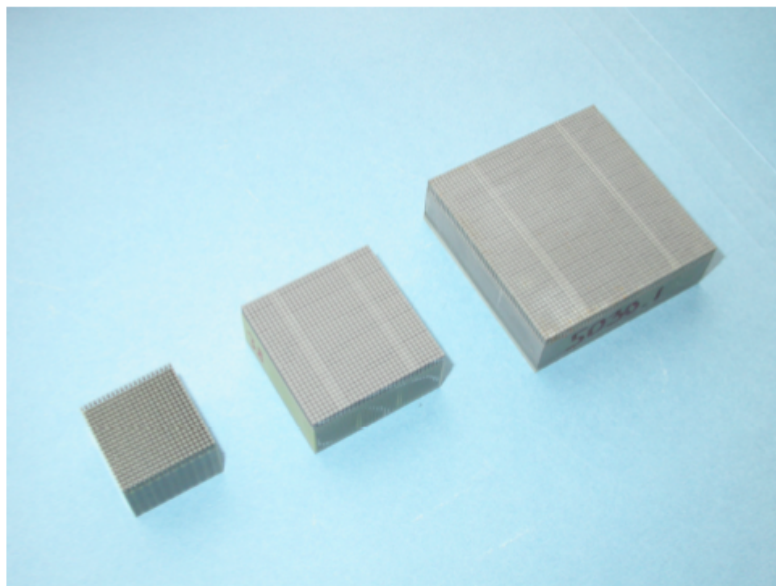
Deformable Mirror Technology

Deformable Mirror Technology demonstrated on the HCIT

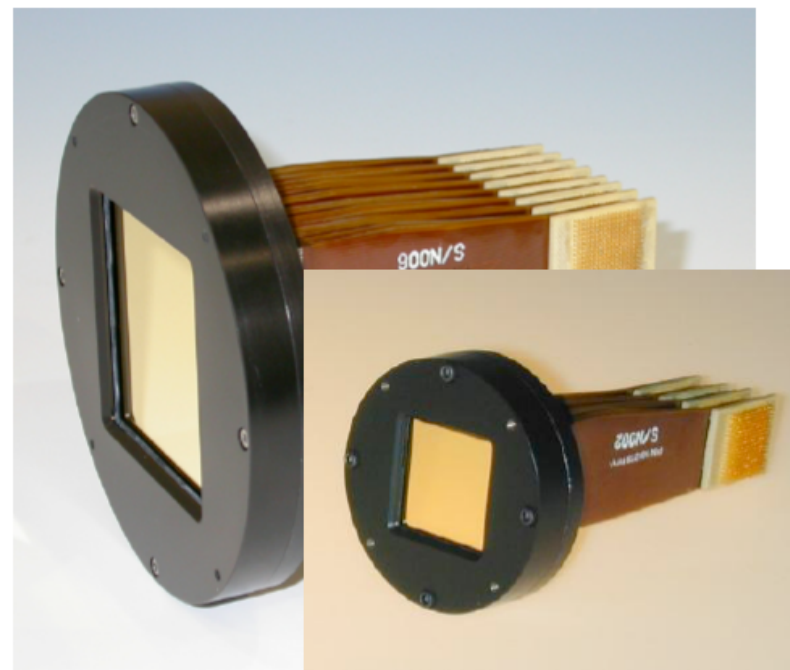
*John Trauger, Amir Give'on, Brian Gordon,
Brian Kern, John Krist, Andreas Kuhnert
Dwight Moody, Peggy Park, Wes Traub, Dan Wilson*

Jet Propulsion Laboratory, Caltech

Deformable mirror development for HCIT

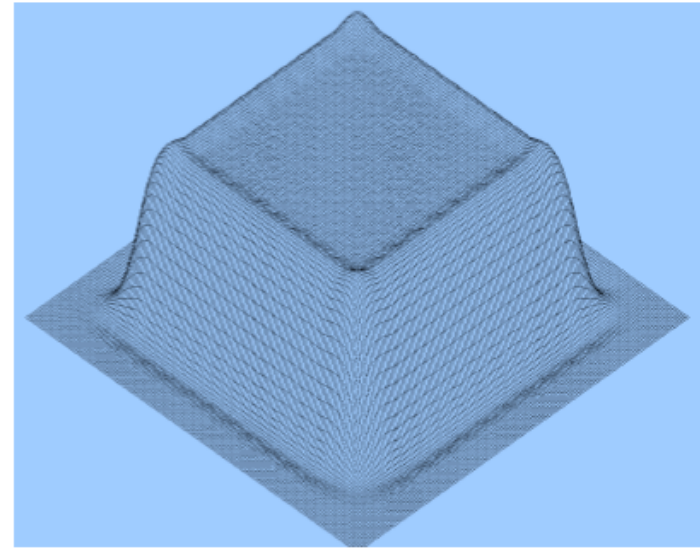
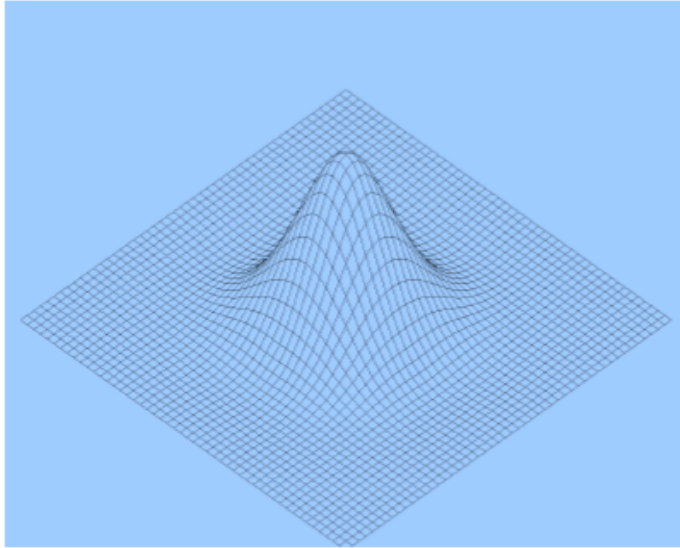


Evolution of monolithic PMN actuator arrays by Xinetics: 21x21, 32x32, and 48x48 arrays. A fused silica facesheet is bonded to the actuator array (top side). Electrical connections (on the bottom side) complete the DM.



DMs delivered to JPL by Xinetics. Larger arrays are formed by bonding modules together: here a 64x64 array is built up with four 32x32 modules. Mirror surface is polished to $\lambda/100$ rms. Surface figure (open loop) is stable to 0.01 nm rms.

DM surface influence function



At left: The empirical surface deformation profile of a single actuator. Grid spacing is 0.1 mm, actuators are positioned in a square array with 1 mm pitch.

At right: Mirror surface predicted by the summation of individual actuator influence profiles in an 11x11 actuator block pattern.

Wavefront Correction Technologies



Scot S. Olivier

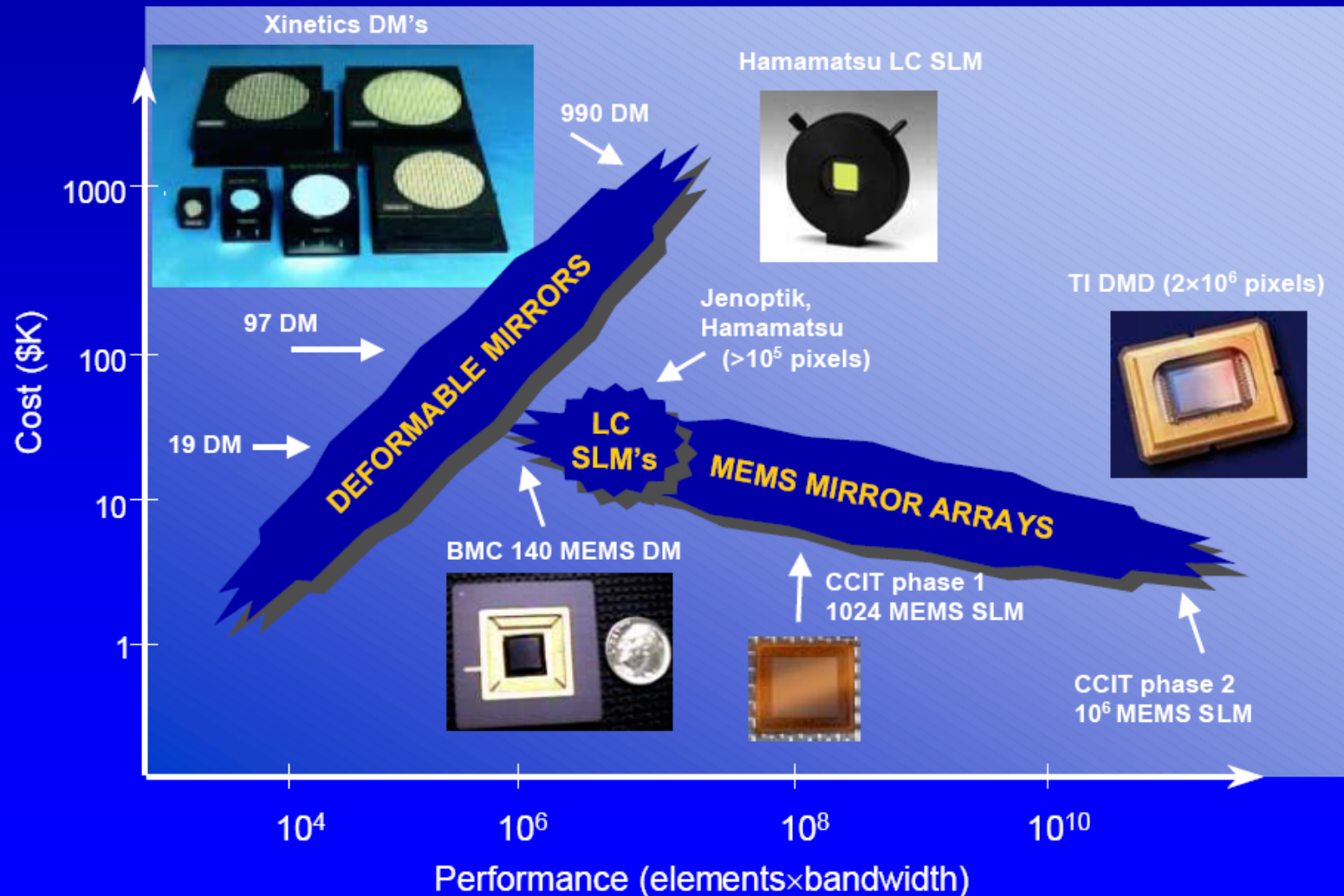


**Adaptive Optics Group Leader
Physics and Advanced Technologies
Lawrence Livermore National Laboratory**

**Associate Director
NSF Center for Adaptive Optics**

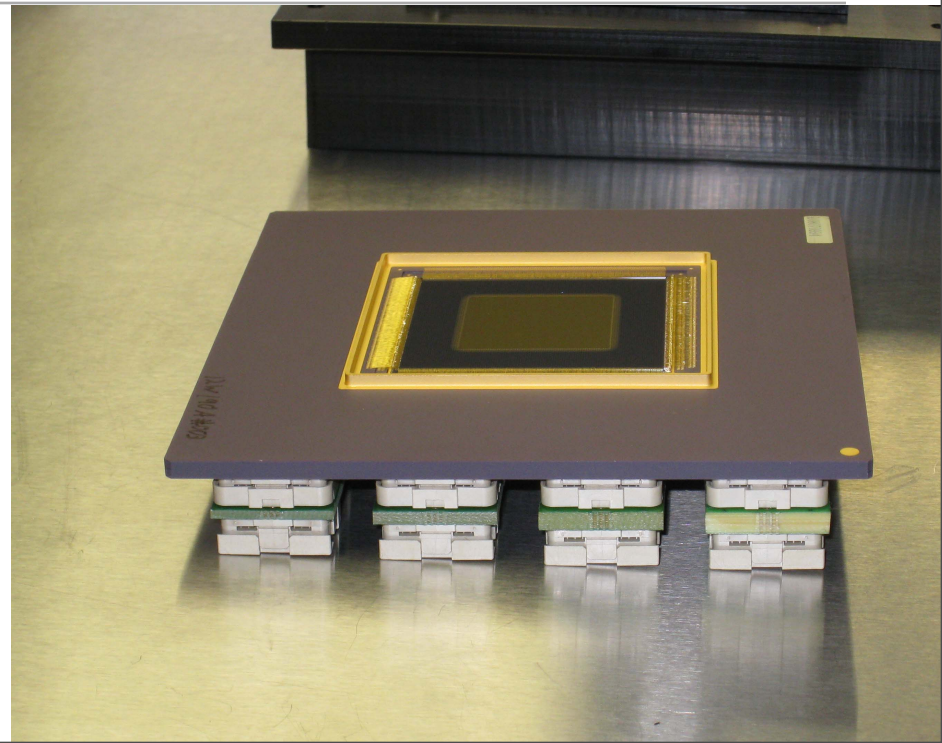
August 7, 2003

New wavefront control devices provide dramatically increased capabilities at lower cost



MEMS Deformable mirrors

Inputs from Boston Micromachines
Dave Palmer (LLNL), GPII





Key MEMS Requirements

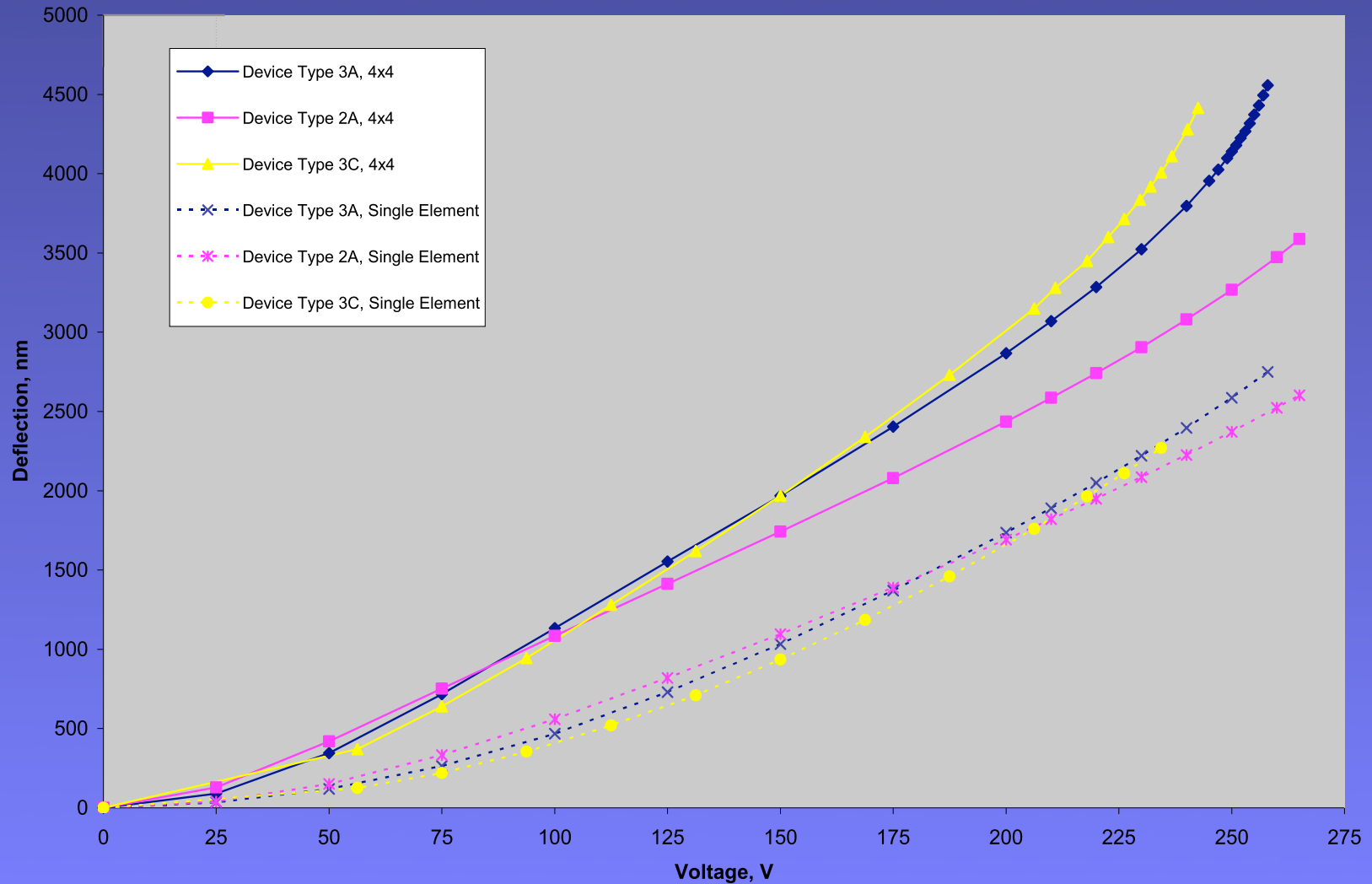


Description	Requirement
Pixel count	4096 (64x64)
Pitch	400 microns
Stroke	3 um, surface, after mirror is flattened
Pixel surface finish (P-V)	< 30 nm (goal: <9 nm)
Flatness over aperture (sphere removed) (RMS)	goal: <70 nm
Neighboring actuator differential stroke	> 1 um, P-V, for a sin wave with a period of 2 actuators
Good actuators	all actuators on a 48 actuator diameter circle must work to full specification
Uniformity of surface reflectivity	+/-1% RMS at all spatial frequencies, measured with a spatial resolution of 1 actuator
Operating temperature, with device still meeting other specs	-5 to 20 degrees Celsius



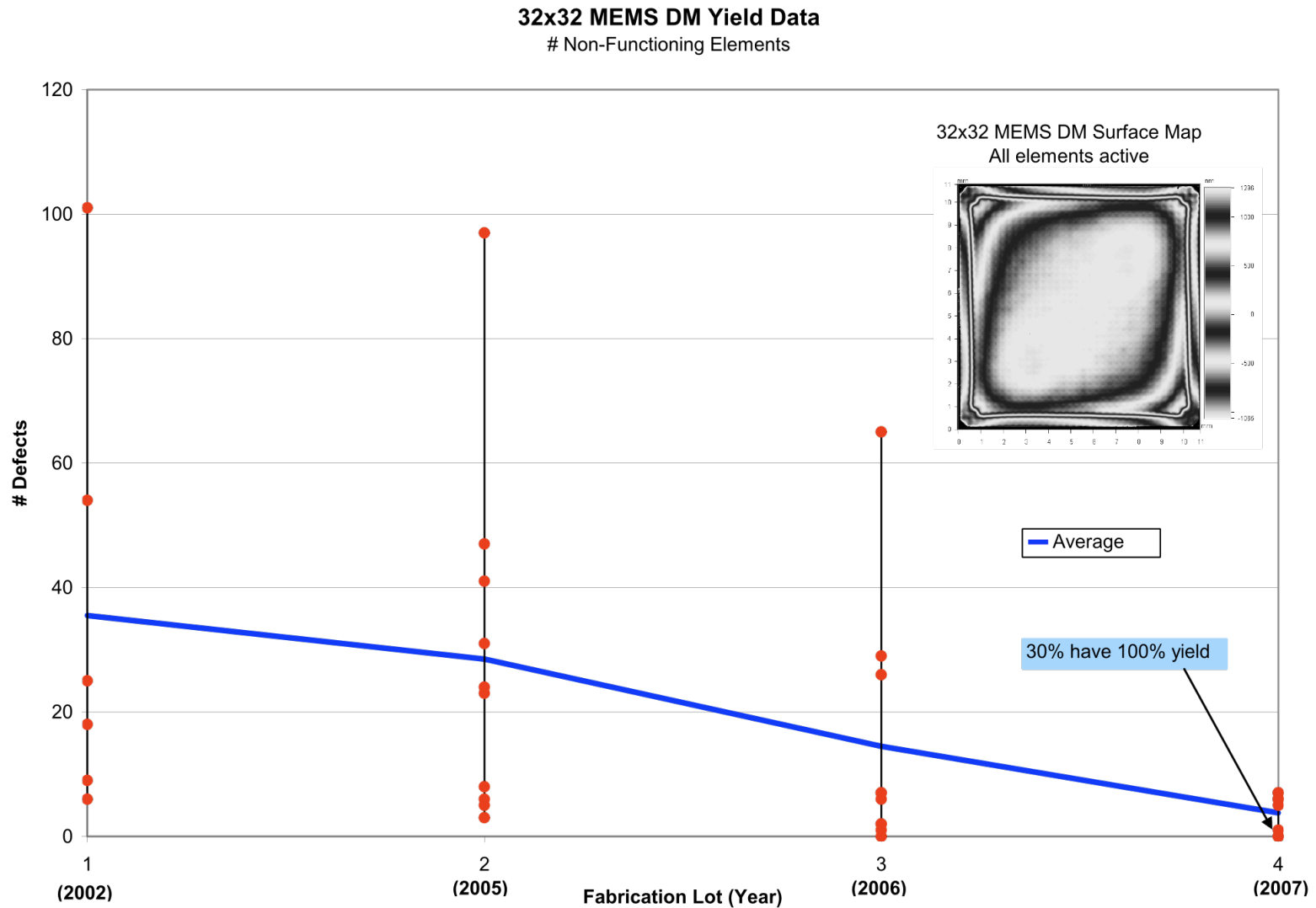
Stroke vs. Voltage For Three Prototype Actuator Designs

Electromechanical Performance of Phase II 4096 DMs





Evolution Of Device Yield (Non-Functional Actuators) As A Function Of Fab Run





Veeco Interferometer Data Of A Single Actuator



Mag: 3.9 X

Mode: PSI

Surface Data

Date: 03/26/200

Time: 09:24:14

Surface Statistics:

Ra: 5.14 nm

Rq: 7.21 nm

Rz: 61.69 nm

Rt: 68.08 nm

Set-up Parameters:

Size: 279 X 258

Sampling: 2.51 μm

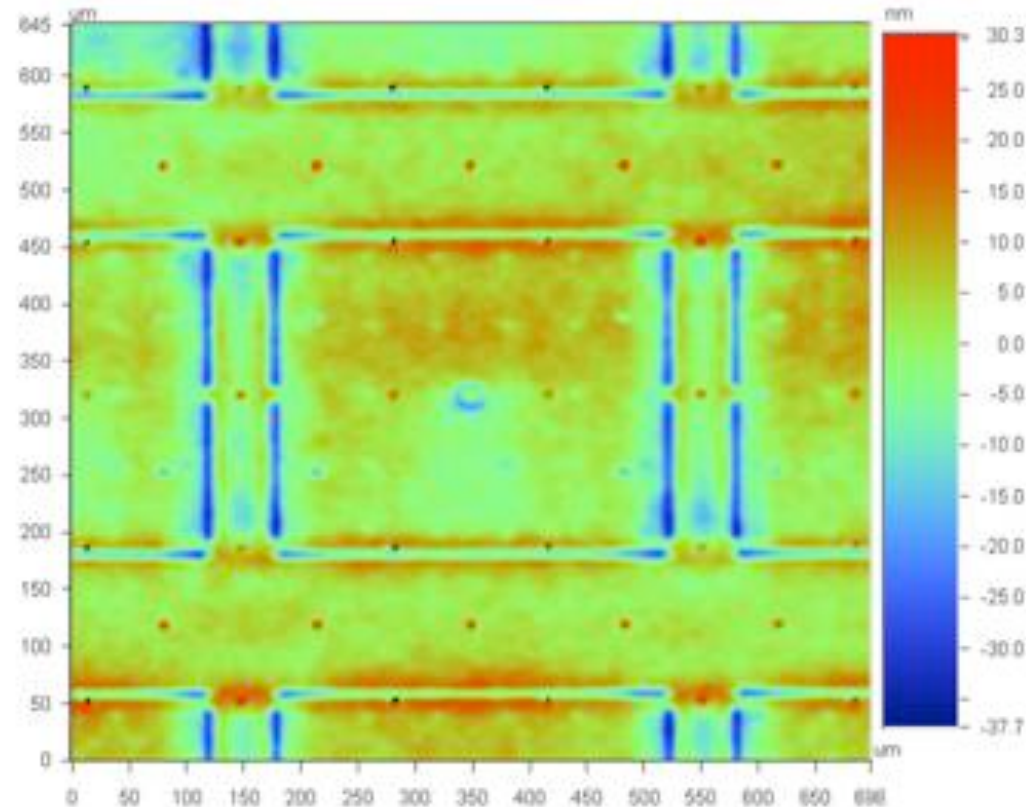
Processed Options:

Terms Removed:

None

Filtering:

None



Title: 12w190A#001

Note: Device Design Type 3a

Materials Science Considerations in the Development of the Coronagraph Deformable Mirror

Robert E. Rudd, Physicist
Lawrence Livermore National Laboratory
7000 East Ave., L-045
Livermore, CA 94550 USA
May 19, 2008

Yield Phenomena

- Silicon is a brittle material and exhibits little plastic flow; however, microscopic plasticity may still be relevant.
- The local shear stress within the membrane changes as the membrane is subjected to:
 - stress due to thermal expansion,
 - forces acting on the support structure, or
 - changes of voltage on the actuators.
- If the local shear stress is sufficiently high, dislocations within the membrane move, causing plastic deformation.
 - This phenomenon is potentially relevant to the question of membrane stability because it is a thermodynamically irreversible process and causes hysteresis.
 - Dislocations terminating on the surface are associated with surface steps, sub-nm scale features. Even before intersecting a surface, the elastic stress fields emanating from a dislocation can cause the displacement of a surface.
- Since polysilicon is strong, it may be that plasticity is not important for the relatively small DM deformations needed in the coronagraph application, but an assessment of the effect of plasticity should be made.

Other Material Effects

- Creep
 - Creep is an irreversible process of plastic flow due to the slow relaxation of stress as a result of stress-driven point defect diffusion.
 - Creep is typically only significant at elevated temperatures or extremely long time scales.
- Elastic Anisotropy
 - Silicon is a cubic crystal in the diamond cubic crystal structure.
 - Single crystal silicon is moderately anisotropic.
 - Polycrystals with a random texture (random grain orientation) is elastically isotropic on length scales that are large compared to the grain size.
 - Given stresses generated during DM operation and a knowledge of the grain structure, it is straightforward to calculate changes in the surface morphology due to elastic anisotropy.
- Anisotropic Thermal Expansion
 - Surface roughening can occur due to anisotropic expansion of the crystal grains even under a uniform heating.
 - This is not an issue for silicon, gold or aluminum, since thermal expansion of cubic

Annealing

- The polysilicon membrane may be annealed prior to the deposition of the metal coating.
 - Such annealing would provide the thermal energy for dislocations to flow, leading to a reduction in the residual stress and the associated dislocation network.
 - Relaxing the residual stress may have the desired effect of reducing local stress and the associated surface deformations at the expense of spreading it across a smooth curvature of the DM, which is more easily countered with the actuators.
- Annealing typically reduces the yield stress of the material, although in the brittle Si this change may not be significant.

BACKUP slides

Coronagraph requirements

Mission type/size	Raw Contrast	Augmented contrast	IWA λ/D	Pointing	Mid Spatial WF stability*	Thermal stability	Optics Quality & Fabrication	Driving science
Internal Coronagraphs								
Ground based 8-m ExAO	1.00E-06	1.00E-07	5	10 mas	5 nm	N/A	x	Young giant planets, debris disks
Ground based 30-m ExAO	1.00E-06	1.00E-08	3	5 mas	5 nm	N/A	x	Formation of planetary systems
Space 0.5-m	1.00E-07	1.00E-07	1	2 mas	1 nm	~ mK	x	debris disks

Mission type/size	Raw Contrast	Augmented contrast	IWA λ/D	Pointing	Mid Spatial WF stability*	Thermal stability	Optics Quality & Fabricatn	Driving science
-------------------	--------------	--------------------	-----------------	----------	---------------------------	-------------------	----------------------------	-----------------

Internal Coronagraphs

Space 1.5-m	1.00E-10 @ 10-20% bandwidth	1.00E-10	~2	0.5 mas	30 pm	~ 0.1 mK	x	Super Earth Jupiters, R = 15
Space 4-m	1.00E-10 @ 10-20% bandwidth	1.00E-11	2-3	0.5 mas	30 pm	~ 0.1 mK	x	Earths Jupiters, R = 40
Space 8-m	1.00E-10 10-20% bandwidth	1.00E-11	3-4	0.5 mas	30 pm	~ 0.5 mK	x	R=100 Spectroscopy on Earths